We are IntechOpen,
the world's leading publisher of Open Access books
Built by scientists, for scientists

6,900
Open access books available

186,000
International authors and editors

200M
Downloads

Our authors are among the

154
Countries delivered to

TOP 1%
most cited scientists

12.2%
Contributors from top 500 universities

CLARIVATE ANALYTICS

BOOK CITATION INDEX

INDEXED

WEB OF SCIENCE™

Selection of our books indexed in the Book Citation Index
in Web of Science™ Core Collection (BKCI)

Interested in publishing with us?
Contact book.department@intechopen.com

Morphological Study of HDPE/Clay Hybrids Synthesized by an Alternative Compatibilization Path

Fernanda Elena Monasterio

Instituto de Investigaciones para la Industria Química (INIQUI)- CONICET, Avda,
Bolivia, Salta,
Argentina

1. Introduction

The control of the factors that influence the internal structure of polymeric materials (crystallinity, miscibility between phases, processing, etc.), is of paramount importance because it is closely related to the outcome of their final properties (Durmus et al., 2007; Sinha Ray & Okamoto, 2003; Franck, n.d.). Therefore, the morphological analysis is essential in order to know the structure-property relationship (Williams & Carter, 2009).

As far as particulate-filled polymer composites is concerned, there are many filling choices to make a material and the use of nanometric fillers such as clays is the most promising one (Sinha Ray & Okamoto, 2003; LeBaron et al., 1999). Due to the fact that these nanomaterials own a higher surface area for the polymer-filler interaction than conventional composites, the effect at the interface will promote changes in the morphology at a nanometric level which can be studied using conventional bulk characterization techniques (Sinha Ray & Bousmina, 2005).

The analysis by Transmission Electron Microscopy (TEM) has been of great help in the characterization of polymer layered nanocomposites (Sinha Ray & Bousmina, 2005; Michler, 2008; Durmus et al., 2007), given that the degree of affinity at the polymer-clay interface is exhibited by the nanosheets dispersion achieved in a TEM image. But this technique, by itself, does not allow a full interpretation of the composites final behavior and it is usually used in combination with other techniques. Among them it can be mentioned the differential scanning calorimetry (DSC) and the rheological analysis that widely reflect distinguishing material features such as miscibility and crystallinity degrees (Faker, 2008; Kim & Lee, 2008).

The DSC allows inferring changes in the polymers internal structure as it registers the transitions taking place in the materials when temperature varies, which is linked to the molecular mobility (Campbell & White, 1989; Rothon, 2003). Regarding clay filled polymers, these are usually superficially modified to reach miscibility leading to a highest intercalation/exfoliation of the multilamellar clay in the polymer matrix. Some authors

(Sinha Ray & Okamoto, 2003; Alexandre & Dubois, 2000; Mai & Yu, 2006) report that polymer structure variations are manifested by changes in the crystallization temperature (T_c) or in the glass transition temperature (T_g) which can be detected by DSC measurements.

On the other hand, rheological tests extensively are used in polymer characterization (Zhang Q. et al., 2004) and they bring important information about processing optimization (C. Wan et al., 2004; Shah & Paul, 2004). Particularly, the structural characterization of filled polymer through low-amplitude oscillatory experiments allows determining the linear viscoelastic properties that describe the material behavior in a condition where the structure remains practically unchanged. These properties are sensitive to the interactions that take place among phases, and to the degree of miscibility reached (Okamoto, 2005; Bretas & D'Avila, 2000; Cassagnau, 2008), due to the fact that the applied strain deformations are small enough to affect the material properties.

In this chapter, several hybrids based on high density polyethylene (HDPE) and montmorillonite are studied. Due to the differences between the hydrophilic natures of these materials, a clay surface modification using difunctional silanes was chosen in order to generate oligomers with hydrophobic lateral groups around the lamellas.

Furthermore, to determine if the final materials behaviors were affected by alterations in the chemical nature of the interphase, alkyl groups were alternated with aryl groups.

On the other hand, transport properties are analyzed aiming to characterize the outcome of the materials at the macroscopic level. In this way, it would be able to know how the use of the structural analysis via TEM can help to understand these behaviors and how, if combined with the two techniques mentioned above, allow a better analysis of polymer composites.

Finally, the results made possible a better understanding of the barrier properties, and some quantitative relations with the structure of the synthesized materials were found.

2. Materials

In polymer/clay systems, the structure at nanometric level (intercalation/exfoliation) depends on the matrix polarity, being more feasible to get better miscibility in polar matrixes. Consequently, compatibilization is required in order to obtain a polyolefin nanocomposite. This implies using copolymers or clay modification by trifunctional silanes or organic ions rendering the nanolamellas more hydrophobic (Durmus et al., 2007; Okamoto, 2005; Malucelli, 2007; L. Wang & J. Sheng, 2005).

Polymer additives were synthesized by treating an organophilic clay (oC) with difunctional silanes, aiming to obtain surface oligomers with side groups compatible to the high density polyethylene matrix, while their backbones share the same clay chemistry. This procedure is proposed as an alternative path for the obtaining of polyolefin/clay nanocomposites and it is based on the methods reported by (X. Zheng & Wilkie, 2003; J. Zhang et al., 2005; C. Zhao et al., 2004).

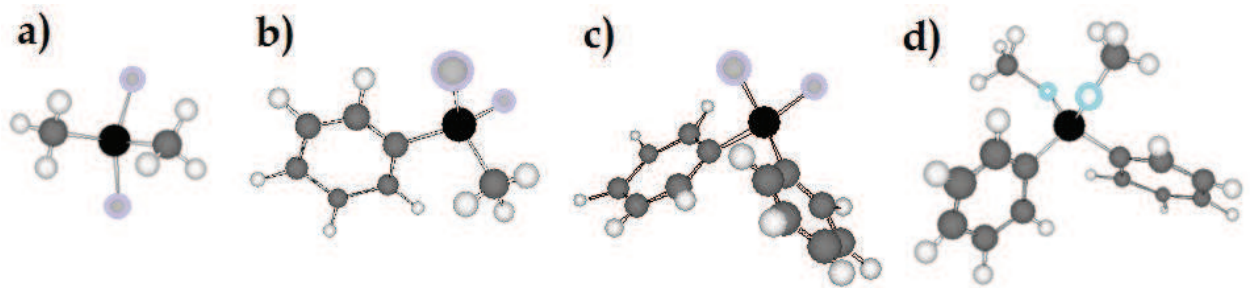The molecular models of the employed silanes are described on Figure 1:

Fig. 1. Molecular simulation of: a) dichlorodimethylsilane (DM)
b) dichloromethylphenylsilane (MP); c) dichlorodiphenylsilane (DP_{Cl}) and
d) dimethoxydiphenylsilane (DP_{OCH_3}).

From these monomers, by means of an in situ hydrolysis, four clays with their respective oligosiloxanes were obtained, named as: oC/DM, oC/MP, oC/DP_{Cl} y oC/DP_{OCH_3}. Subsequently, they were mixed with HDPE by melting process thus each composite contained ~3%wt clay. The preparation conditions and the results from X-ray diffraction, Fourier transform infrared spectroscopy and non-oxidative thermal degradation of the clays and the polymeric materials can be found in Monasterio et al. (2010, 2011) and Monasterio & Destéfanis (2011).

To systematize the analysis of the HDPE/clay materials, the collected data was split in two groups according with the criteria described on Table 1:

Group	Criteria	Hybrid
I	Oligomers obtained from the same reactive group (-Cl) with different side groups	PE-oC/DM PE-oC/MP PE-oC/DP_{Cl}
II	Oligomers with equal side groups (-C_6H_5) obtained from different reactive groups	PE-oC/DP_{Cl} PE-oC/DP_{OCH_3}

Table 1. Polymeric systems studied in this chapter.

In the following sections it must be taken into account that the prepared PE composites contain equal clay percentage, and since it is the same polymer matrix and the same inorganic multilayered material, the changes detected by the above mentioned techniques will be associated to the effects obtained by the modifying species present in the different interphases generated on each clay.

To perform a more detailed analysis of the oligomers effects in the interphase, the hybrids with sC and oC are included.

3. Structural characterization via TEM

Before incorporating the additives (clays) into the HDPE, they were analyzed by TEM. Each of the samples was sonicated in ethanol. The resulting suspension of the product in the solvent was settled for approximately 20 minutes and then, a drop of the dilute suspension was placed onto a coated copper grid. The solvent evaporated from the grid, leaving a thin-layer of each of the products on the grid. Figure 2 shows the photographs of three of the used clays.
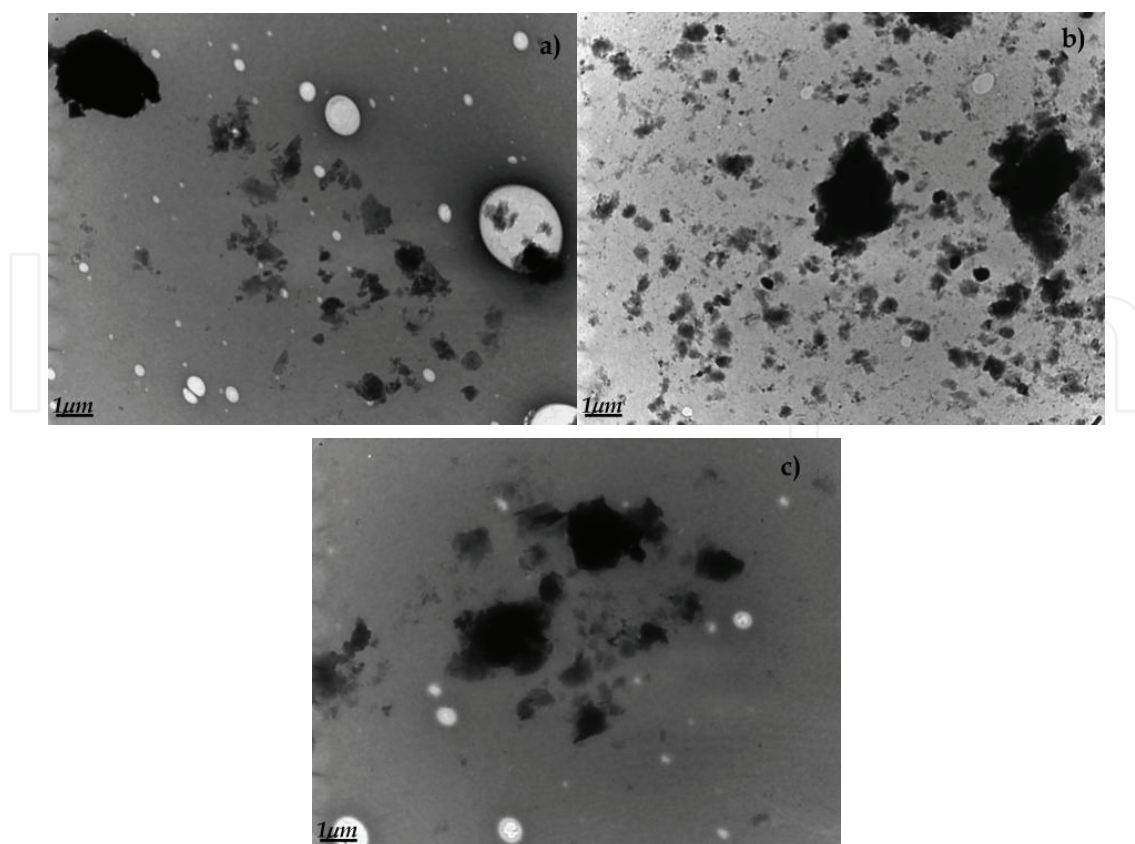
Fig. 2. TEM images of a) oC, b) oC/DM y c) oC/DP$_{OCH_3}$ performed on a JEOL100 CX II (10000×). The whiter ovals are part of the defects on the support films.

In general, particulate materials of different sizes were visualized. In addition, tonality changes were observed which are related to the mass-thickness contrast, pointing out differences in the particle thickness or the composition. The thinner particles (light grey) were associated with clay sheets.

The clays containing oligosiloxanes tend to form clusters. In all cases, agglomerates superior to 1 μm were observed but they presented different appearances. In Figure 2a), it has a black color while similar sized agglomerates in the other samples are surrounded by lighter grey particles. This can be the result of higher clay dispersion caused by the in situ generation of oligomers into the organophilic clay. These results are in agreement with previous scanning electron microscopy studies of these additives (Monasterio et al., 2010).

Thin sections (~60nm) cut by means of a cryoultramicrotome were obtained for the HDPE/clay hybrids morphological analysis. Cryoultramicrotomy is a standard method often used with low T$_g$ polymers (e.g. HDPE T$_g$=-125°C) (Kaufman & Falcetta, 1977), because it provides thin sections that are free from artefacts. Hence it is possible to carry out a correct interpretation of the actual composite morphology (Michler, 2008). The visualization was performed at high acceleration voltage (100kV), which improves the resolution and reduces the scattering cross-section to protect the specimens which are sensitive to electronic radiation (Williams & Carter, 2009). It must be mentioned that SEM photographs of these composites (Monasterio et al., 2011; Monasterio & Destéfanis, 2011) revealed that clays (with or without surface treatment) achieved a good distribution inside

HDPE. In order to guarantee representativeness, TEM images with different magnification were captured (10000×, 40000× and 50000×).

Figure 3 is showing that modification of the chemical nature of siloxane oligomers used as compatibilizer induced differences in the hybrids internal structure.
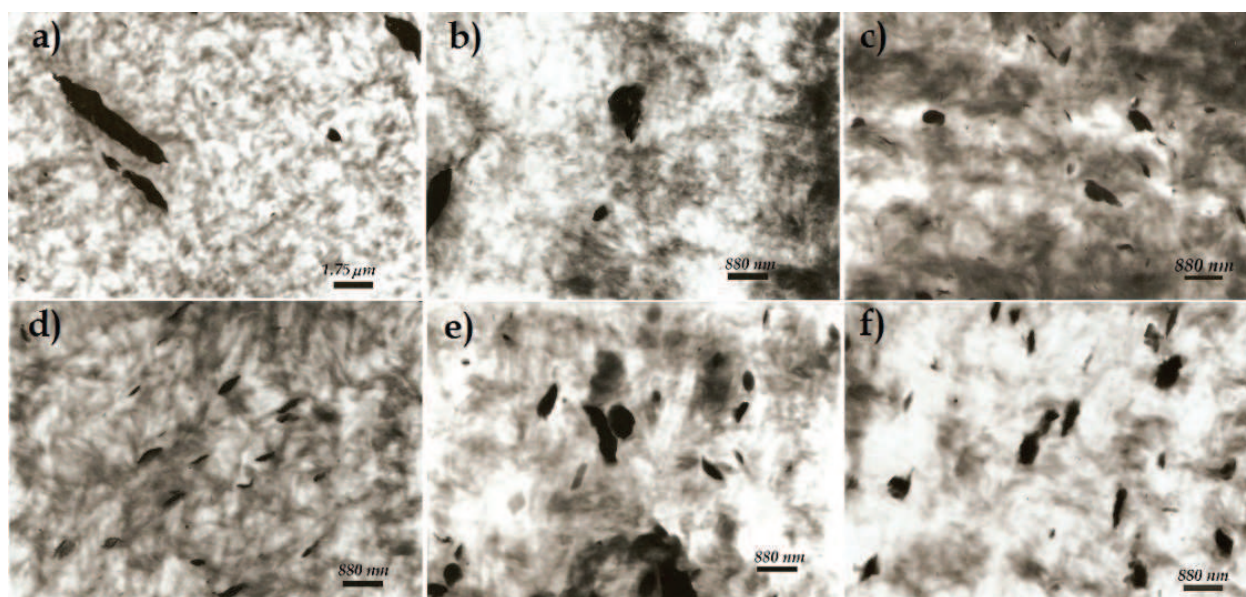

Fig. 3. TEM micrographs of a)PE-sC, b) PE-oC, c) PE-oC/DM, d) PE-oC/MP, e) PE-oC/DP$_{Cl}$ and f) PE-oC/DP$_{OCH_3}$ (Reprinted from Monasterio et al., Copyright (2010) The Mineralogical Society, U.K.).

Dispersed particles of micrometric size were observed in PE-sC and PE-oC. While oligosiloxanes modified clays exhibited a major stacks disaggregation. Taking into account group I (Table 1), PE-oC/MP presents the best dispersion/distribution (particles thickness < 200nm) while the rest of the composites show agglomerations. For group II, where the treated clay composition is basically the same, PE-oC/DP$_{OCH_3}$ exhibited better dispersion of the filler (particles thickness < 500 nm).

On the other side, X-ray diffractograms reported before (Monasterio et al., 2011; Monasterio & Destéfanis, 2011) showed intercalation/exfoliation for PE-oC/MP and PE-oC/DP$_{OCH_3}$, and they were coextensive with that observed in TEM photographs. Although PE-oC/DM and PE-oC/DP$_{Cl}$, had better delamination than PE-sC y PE-oC, they exhibited 'stacking recovery'.

In conclusion, the decreasing dispersion order was PE-oC/MP, PE-oC/DP$_{OCH_3}$, PE-oC/DM, PE-oC/DP$_{Cl}$, PE-oC, PE-sC. Specially, the morphology obtained in PE-oC/MP is similar to that reported by TEM images by Zhang et al. for PE and PP nanocomposites (J. Zhang et al., 2005). Consequently, the proposed oligosiloxane treatment could be considered as an alternative for compatibilization.

4. Structural characterization via rheological analysis

Rheological behaviors in oscillatory regime were determined in a rheometer TA AR2000 of parallel plates (D=25 mm, h= 1 mm) at 200°C in N$_2$ atmosphere. Before measuring, each

sample underwent a relaxation at an angular frequency of 5 rad/s. Results were plotted using the 'frequency domain phasor representation' (Figure 4). The locus of a phasor is known as the 'digital fingerprint' of a material. This plot summarizes the values of storage (G') and loss (G") moduli and the phase angle (δ).

From this representation, an increase of clay-polyolefin compatibility was inferred. It can also be noticed that PE was above the other values, whereas PE with sodium clay values were below the other hybrids. PE-oC behavior is near of that described by PE-sC while materials containing oligosiloxanes presented a behavior closing to pure PE.

On the other hand, not only were noticed changes for the materials with different reactive leaving groups (group II) but also for those with different side groups (group I). At low frequencies, composites containing oligomers presented lower G' and G'' values than PE. Phase angle were between 30 and 60° which denotes the composites viscoelastic nature.

Figure 5 illustrates the curve of viscosity as a function of the frequency where a pseudoplastic behavior for pure HDPE and hybrids was observed. This is due to the fact that the input shear energy tends to line up random oriented molecules or particles and to disaggregate any large clay stacks, thereby reducing the overall hydrodynamic drag, which in turn reduces the dissipation of energy in the fluid and the viscosity (Punnarak et al., 2006; D. Chen et al., 2005; TA Instruments, (RN-9B)).
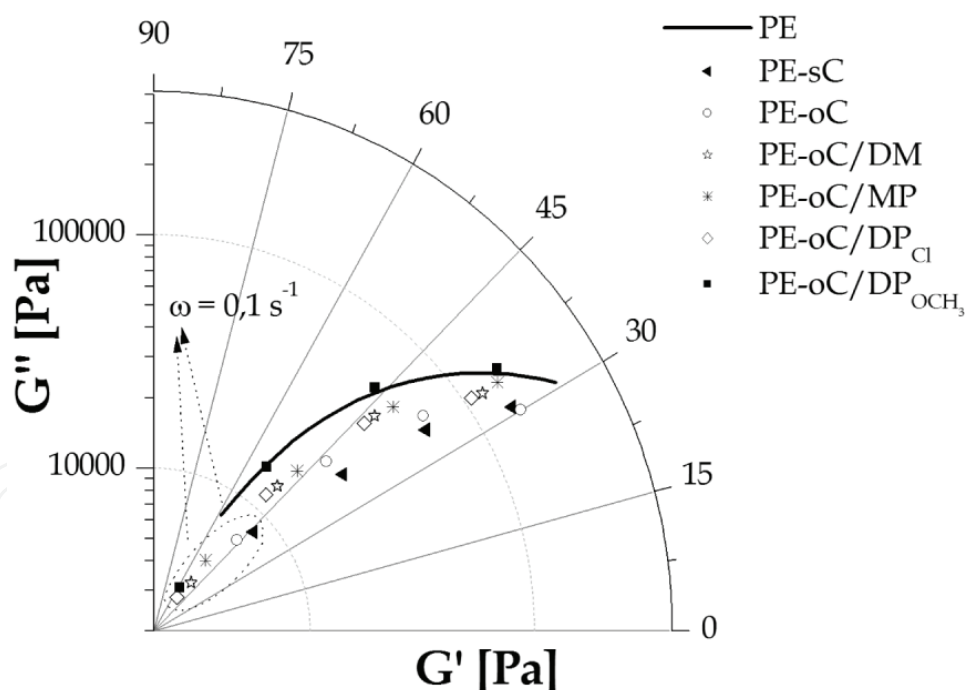

Fig. 4. Phasor representation of pure PE and PE/clay composites at ω=0.1,1,10,100 rad/s.

Unlike other works describing an increase in viscosity due to the addition of filler into the polymeric matrix (Cassagnau, 2008), the materials modified with clays showed lower values than that corresponding to HDPE. In the case of PE-sC and PE-oC, one of the factors that could give rise to this behavior would be the diminution among PE macromolecules interactions due to the presence of clay tactoids.
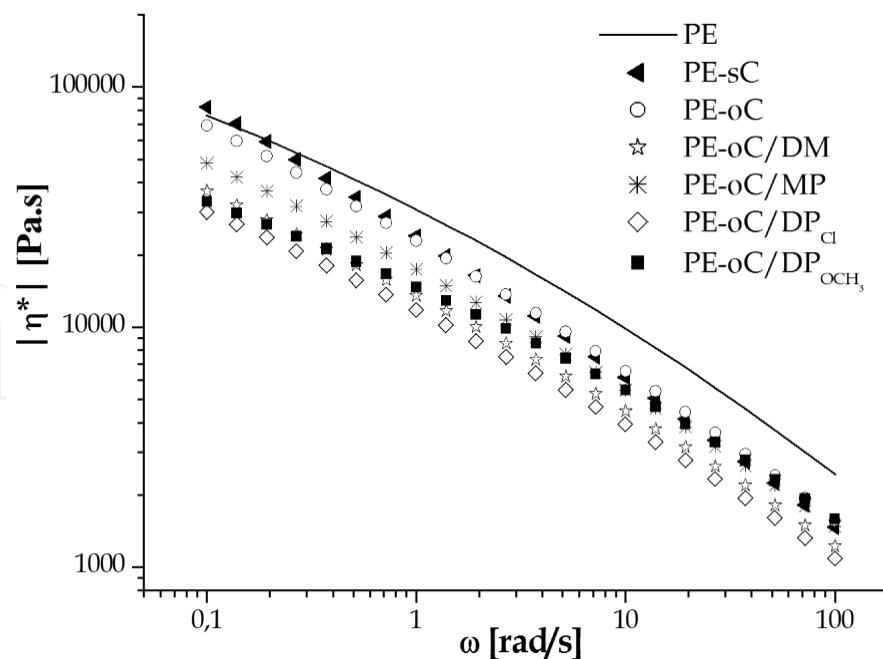
Fig. 5. Complex viscosity vs frequency for neat and clay-filled HDPE.

For hybrids filled with silane treated clays, oligomers would diminish the average molecular weight affecting the viscosity (Billmeyer, 1988). Among siloxane treated hybrids, it is observed that at low frequencies the highest viscosity is for PE-oC/MP, followed by PE-oC/DM and finally by PE-oC/DP$_{OCH_3}$ and PE-oC/DP$_{Cl}$. Probably this is a consequence of the effects caused by oligomeric species obtained during the in situ hydrolysis of each monomer introduced into oC.
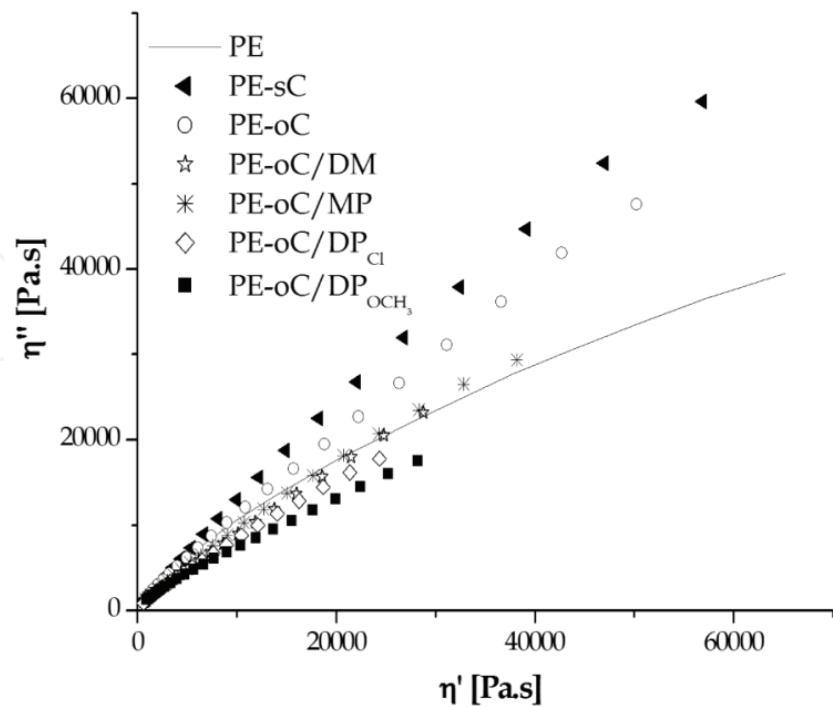

Fig. 6. Cole-Cole plot showing clays effect in PE hybrids miscibility.

The Cole-Cole viscosity representation (Figure 6) was also analyzed to know the miscibility among the hybrids components. The curves proximity to a semicircular shape indicates higher miscibility and the deviations respond to a component interaction reduction (Ahmed et al., 2010). In this way, it was detected that both sC and oC did not reach a good compatibility with the polymer matrix, while the other siloxane treated clays composites showed miscibility with PE.

A deep structural analysis can be performed by using the van Gurp-Palmen plot which provides information about the length and amount of branches in a sample, and the molecular weight distribution (Lohse et al., 2002; Schlatter et al., 2005).
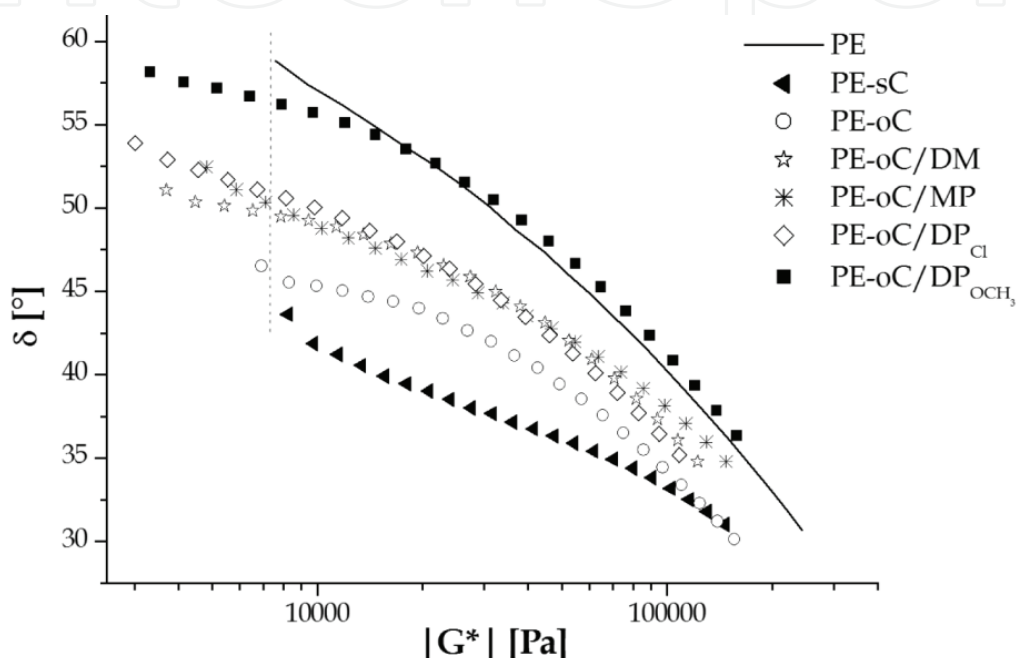

Fig. 7. Phase angle (δ) vs. the absolute value of the complex modulus |G*| of HDPE/clay hybrids.

The dashed line in Figure 7 was pointed out for polydispersion comparison taking pure PE as reference. As was expected for PE-sC and PE-oC there are not variations. Nevertheless, for group I, it was observed the following polydispersion decreasing order: PE-oC/MP, PE-oC/DM and PE-oC/DP$_{Cl}$. Regarding group II, PE-oC/DP$_{OCH_3}$ and PE-oC/DP$_{Cl}$ exhibited similar behaviors.

These results are in agreement with the GPC results (Monasterio et al., 2010, 2011) (Table 2) and they explain the above mentioned viscosity decrease (Figure 5). Interestingly in group II, dimers were synthesized and the chemical nature of the interaction was similar. However, different behaviors were detected. In one of the cited papers, it was made a comparative analysis between PE-oC/DP$_{Cl}$ and PE-oC/DP$_{OCH_3}$ behaviors. From it, it was possible to conclude that the differences between the mechanisms during the synthesis of the oligosiloxane surface modified clays affected their further interactions when being added to PE. Basically, the difference between both additives lies in the degree of coating achieved on clay platelets.

Further analyses were carried out and their values are shown in Table 2. Even though the above graphics give an idea of the information of each material behavior, the Table data offer specific quantitative results of each system which later will be associated with transport properties.

	G_{cop} [kPa]	G_N^0 [kPa]	G′ slope	PDI
PE	38.1	841.1	0.73	
PE-sC	5.5[*]	792.6	0.52	
PE-oC	8.6	612.1	0.56	
PE-oC/DM	23.3	523.6	0.60	1.10
PE-oC/MP	20.3	681.4	0.63	1.32 and 2.37
PE-oC/DP$_{Cl}$	22.1	477.7	0.66	1.26
PE-oC/DP$_{OCH_3}$	45.9	638.8	0.69	1.08

Table 2. Rheological characteristics of HDPE and HDPE/clay hybrids. ([*]Extrapolated value. G_N^0: Plateau modulus calculated from extrapolation on van Gurp-Palmen plot (García-Franco et al., 2006). PDI: polydispersity index of the oligomers extracted from the oligosiloxane clays before their incorporation to PE. Values obtained by GPC measures).

The crossover point modulus (G_{cop}) indicates the transition from a solid-like behavior to a liquid-like behavior. Its value can provide the qualitative information about the average molecular weight (M_w), the degree of branching and the molecular mass distribution (Yang, Q. et al., 2009; Ahmed et al., 2010). Reminding that the matrix is the same in the analyzed materials (HDPE), it can be observed that G_{cop} has had a significant change according to the surface treatment applied on each clay. When polydipersion of the modifying oligomers increase, the G_{cop} values decrease. The low values presented by PE-sC and PE-oC are associated to poor interfacial adhesion.

Group I hybrids presented similar values among them and a more elastic (liquid-like) behavior than PE, but in group II it is evident that PE-oC/DP$_{OCH_3}$, in spite of its similarity with PE-oC/DP$_{Cl}$, it shows a value even higher than neat PE, which it make expect differences in the internal structures of these materials.

It was also analyzed the effect of the clays on the plateau modulus (G_N^0). This value is defined by the Equation 1 (Rose et al., 2007):

$$G_N^0 = \frac{b.R.T.\rho}{M_e} \qquad (1)$$

where:

b: coefficient equal to 1, according to Ferry, and equal to 4/5, according to Doi and Edwards,
R: is the ideal gas constant,
T: is the absolute temperature,
ρ: is the polymer density, and
M_e: is the entanglement molecular weight.

So G_N^0 bring information about the entanglement spacing of a polymer melt and the entanglement molar mass. In the case of filled materials, this value could be associated with

temporary crosslink between the surface of the particles and the polymer (Gacitua E. et al., 2005). In PE-sC the clay has not any organic species as compatibilizer, so the lower value it might be because no interaction takes place between its surface and the long HDPE chains. It is evident that the presence of intergallery organic ions in oC is not enough to improve the interaction with the matrix. Not only does the G_N^0 not increase, but even more it is inferior to PE-sC value. This behavior could be due to oC tendency to easily delaminate (compared to sC), which would increase the amount of low compatibility particle dispersed in the matrix.

The treatments with silanes had different effects, being PE-oC/DP$_{OCH_3}$ and PE-oC/MP the composites with higher values taking PE-oC as reference, whereas PE-oC/DM and PE-oC/DP$_{Cl}$ had the lowest values. Evidently, these behaviors are not directly affected by the chemical nature of the side groups. It would be more appropriate to take into account the coating generated by the dissimilar species over the clays to explain these results. Therefore one can think in an oligomer network generated around the sheets (or stack of sheets).

In oC/MP there are trimers and longer chains that can lead to an intricate coating, just like oC/DP$_{OCH_3}$ which has a higher proportion of dimers outside of clay galleries (compared to oC/DP$_{Cl}$). So, inside HDPE matrix is more probable that these networks give rise to temporary anchoring that would improve its interaction. In the case of oC/DP$_{Cl}$, the low dimers concentrarion on the surface would prevent the network formation, and although oC/DM has longer oligomers (mostly pentamers), the rigidity and spatial complexity of the –CH$_3$ group is smaller than the phenyl group, which would explain that this clay does not have such capability to 'entangled' the PE macromolecules. This would also explain the PE-oC/DM and PE-oC/DP$_{Cl}$ 'stacking recovery' tendency mentioned above.

Nevertheless, the G_N^0 values (Table 2) were below the pure PE value, evidencing that despite of the improvements got at the interphase there would be more free volume.

G' values at the terminal zone give information about matrix-filler interaction (Wang, K.H. et al., 2002). Due to PE-sC hybrid did not have any compatibilization it is expected to show the lowest value, as in the system coexist hydrophilic and hydrophobic components.

The Na$^+$ exchange with hexadecyltrimethylammonium ion provided a slight improvement in the interface interaction. Only after the second treatment of the clays in order to generate oligosiloxanes, it was possible that these additives increase their slopes, which is associated to an increase in compatibility. Moreover, the G' slope for PE-oC/DP$_{OCH_3}$ presented a value near to the pure polymer, which is in agreement with the behaviors observed in Figure 6 and which would indicate an improvement in polymer-clay interactions.

5. Structural characterization by DSC

Semicrystalline polymers like HDPE give information about the behaviors of the amorphous and crystalline phases through T_g (glass transition temperature) and T_m (melt temperature) or ΔH_m (melting enthalpy), respectively (Kaufman & Falcetta, 1977). In the analyzed materials, measurements were carried out in a temperature range above the T_g (-50 to 150°C).

The determinations were performed on a DSC Q200 equipment from TA Instruments (coupled with a refrigerated cooling system), equipped with modulated DSC software, which allows the application of a sinusoidal heating programme superimposed to the normal linear temperature ramp (Verdonck et al., 1999; TA Instruments (TS-25)).

$$\frac{dH}{dt} = C_p \frac{dT}{dt} + f(T,t) \tag{2}$$

where:

$\frac{dH}{dt}$: is the Total Heat Flow due to the linear heating rate.

C_p: is the Heat Capacity of the Reversing Heat Flow Component.

$\frac{dT}{dt}$: is the measured heating rate, which has both a linear and sinusoidal (modulated) component.

$f(T,t)$: is the Kinetic Component of the Total heat flow and is calculated from the difference between the Total signal and Heat Capacity Component. (Non-reversing component)

$C_p \frac{dT}{dt}$: is the Reversing Heat Flow Component of the Total Heat Flow.

This analysis (Equation 2) allows the deconvolution of the total heat flow signal into 'reversing' and 'non-reversing' contributions. Total Heat Flow due to the underlying heating rate it is equivalent to standard DSC signal at the same average heating rate (De Meuter et al., 1999), and the results obtained from these curves are described in Table 3. Compared with pure polymer, hybrids did not presented significant changes for T_m, T_{onset} and degrees of crystallinity, which are in agreement with that reported by other authors in HDPE/clay systems (Gupta & Bhattacharya, 2008).

	T_m [°C]	T_{onset} [°C]	ΔH_m [J/g]	Crystallinity degree [%]
PE	129.86	123.85	213.9	73.8
PE-sC	130.09	121.82	193.0	68.6
PE-oC	130.40	121.81	192.0	68.2
PE-oC/DM	130.31	122.17	197.4	70.2
PE-oC/MP	129.75	122.36	202.4	71.9
PE-oC/DP$_{Cl}$	130.47	122.09	188.8	67.1
PE-oC/DP$_{OCH_3}$	130.10	122.18	194.1	69.0

Table 3. Results from DSC non-isothermal analysis.

However, regarding the degree of crystallinity it is noticed that clay addition (with or without oligomers), had a slight plasticizing effect as it affected the chain regularity, inhibiting crystallization.

To have a better insight of composites structure, each component of the Total Heat Flow was analyzed. The advantage of modulated signals is the possibility of separate overlapping phenomena (overlapping transitions such as melting/recrystallization in semi-crystalline materials). This complementary information enables a more detailed study of complicated material systems (Verdonck et al., 1999; Coleman & Craig, 1996). Special care must be taken in the selection of modulation technique as it will affect data interpretation (Schawe, 1995), here it was adopted the model proposed by TA Instruments (Thomas, 2005).

It must be pointed out that the melting process is partially retrieved in the reversing heat flow as well as in the non-reversing heat flow signal, and moreover the fraction of melting in both of these signals depends on the experimental conditions (Coleman & Craig, 1996; Verdonck et al., 1999). For that reason, experimental conditions (heating rate and period) for the hybrids studied were chosen guaranteeing enough modulation cycles during the transition of interest.

In order to avoid degradative processes overlapping during result interpretation, TG-DTG analyses over the assessed temperature range were analyzed (Monasterio et al., 2011; Monasterio & Destéfanis, 2011) and no degradation was observed.

Signal deconvolution shows that the main contribution corresponds to the non-reversing component, which exhibited a similar behavior to that of Total Heat Flow signal, even the maxima from both curves coincided. Regarding reversing signals (Figure 8), the curve corresponding to pure polymer showed a small exothermic peak above T_m and an endothermic peak below the T_m. They can be associated to simultaneous melting-crystallization occurring during heating, until complete melting.
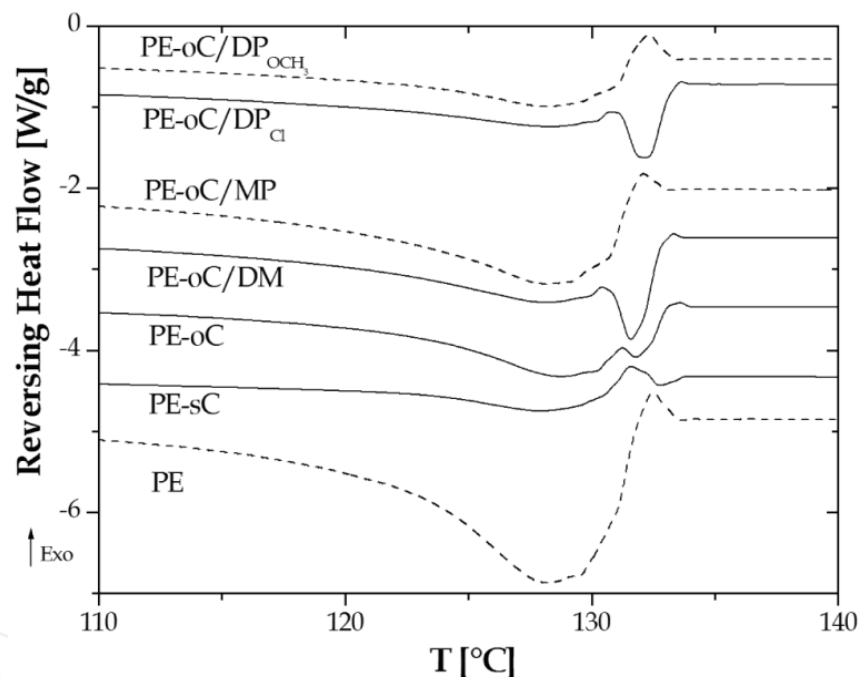

Fig. 8. PE and PE/clay hybrids 'reversing' components. Heating rate was 1°C/min and was modulated by a sinusoid with amplitude ±0,16°C and period 60 s. Nitrogen was used as a purge gas. Samples thermal history was erased by a first heating-cooling cycle.

On the other hand, despite their low clay percentage, composites showed changes compared with the curve above mentioned. Evidently, there are alterations into molecular ordering linked to the different features provided by the interphases that lead to different heat absorption-release mechanisms in the zone near to 130°C. In general it was observed a decrease in the endotherm below to 130°C and in most cases it was seen an endothermic peak above this temperature. PE-oC/MP (group I) and PE-oC/DP$_{OCH_3}$ (group II) behaviors must be underlined because they are similar to PE behavior, and for that reason they were represented by dashed lines.

Based on this, it would be expected that values in a Table 3 would be closer for these hybrids. Nonetheless, values did not match with the tendencies described by reversing curves, as crystallinity degree estimation involves information provided by conventional DSC curves. In this way, it is observed that crystallinity does not entirely reflect the material information related to the variation of the interphase characteristics.

Comparing Table 3 with the behaviors registered in Figure 8, a better interpretation of results can be carried out. PE-oC and PE-sC presented similar crystallinity values, thus alkylammonium chains are not enough to produce significant changes. Meanwhile, it is observed that composites containing oligomers with methyl side groups (similar to HDPE) presented a closer value to pure polymer. Moreover, the highest crystallinity of PE-oC/MP can be explained by the phenyl side group which increases free volume and according to the spatial configuration acquired, it could give to HDPE less spatial restrictions.

Finally, PE-oC/DP$_{Cl}$ and PE-oC/DP$_{OCH_3}$ had low flexibility oligomeric species, which would explain the crystallinity decrease because it would be a hindrance to achieve oligomer-HDPE interfacial ordering. The highest value of PE-oC/DP$_{OCH_3}$ can be the result of the already mentioned difference in the clay coating, allowing a better ordering with HDPE chains at the interphase.

A better understanding of oligomeric species mobility can be performed by reversing heat capacity (Rev Cp) curves (Figure 9) as there are associated to structural changes (Coleman & Craig, 1996).
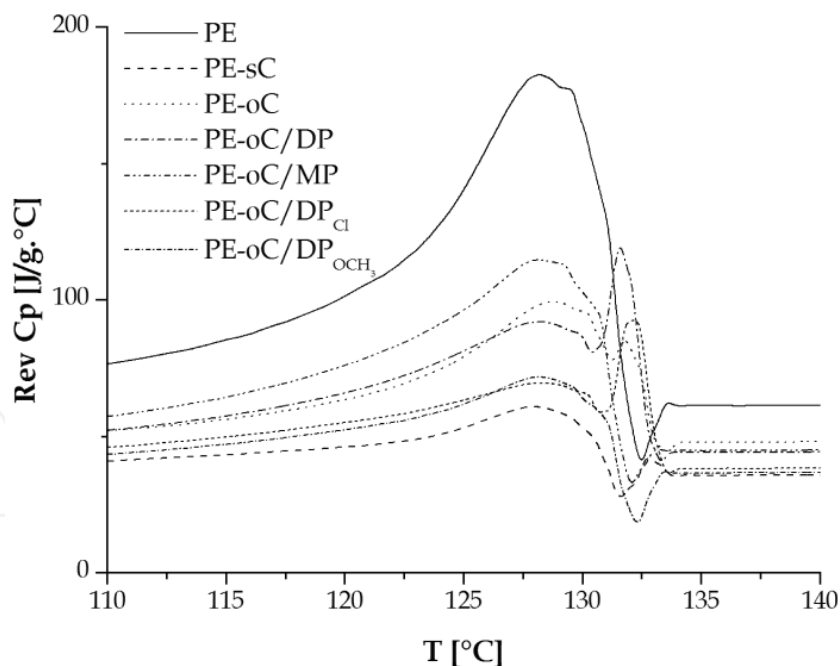

Fig. 9. Reversing Cp comparison of the studied composites in the range of 110 to 140°C.

As it was pointed out, DRX analysis of these polymers (Monasterio et al., 2011; Monasterio & Destéfanis, 2011) corroborated the dispersion exhibited in Figure 3 (TEM) showing exfoliation for PE-oC/MP and intercalation for PE-oC/DP$_{OCH_3}$. Both composites show similar behaviors to that of HDPE, perhaps the cause is that oligomeric species provide

tridimensional arrangements that permit macromolecules to achieve highly free movements near the dispersed particles interphase. For the remaining hybrids, dispersions and interphase features were different.

Therefore, the peaks above 132°C for PE-oC, PE-oC/DM and PE-oC/DP$_{Cl}$ would be the result of clay confined species that only can manifest themselves after complete HDPE melting.

6. Transport properties

Until now, due to alterations at PE-clay interphase, changes were detected in the structure of the studied hybrids and therefore, it will be analyzed if such changes have led to any effect on barrier properties. There are several papers where these macroscopic properties could be modified by handling polymer morphological features such as orientation and degree of crystallinity, as both are linked to chain packing efficiency (Koros, 1990).

Bearing in mind that HDPE is a semicrystalline material, it must be outstood that transport through these polymeric systems are usually analyzed on the basis of a simple two phase model, consisting of a dispersed impermeable crystalline phase in a permeable amorphous matrix (Koros, 1990). In addition, a more complex scenario is given by filled composites as they have clay, which effect will depend on the aspect ratio provided according to the degree of tactoids delamination.

Other factors that influence these properties are the size and chemical nature of penetrating species (Koros, 1990). For the following experiences, apolar molecules of different sizes were employed.

6.1 Gas permeation

Gas permeation measurements were performed on standard permeation equipment. Permeability values of CH_4 and CO_2 were determined at a pressure of 4 bar and a temperature of 30°C.

Table 4 shows higher CO_2 permeability compared to CH_4 permeability, due to higher condensability of CO_2. For unfilled PE, the CO_2/CH_4 permeability rate is near to four, similar to that reported by Stancell (Tobolsky & Mark, 1971).

Sample	CH_4		CO_2	
	P [barrer]	P/P$_{PE}$	P [barrer]	P/P$_{PE}$
PE	0.772	1	3.433	1
PE-sC	0.623	0,807	1.980	0,577
PE-oC	1.512	1,959	6.566	1,913
PE-oC/DM	0.835	1,082	2.551	0,743
PE-oC/MP	0.786	1,018	3.667	1,068
PE-oC/DP$_{Cl}$	0.666	0,863	2.324	0,677
PE-oC/DP$_{OCH_3}$	0.620	0,803	2.357	0,687

Table 4. Transport properties for PE and PE/clay hybrids. (P$_{PE}$: Permeability of pure HDPE)

From a simplified model proposed by Nielsen (1967) (Equation 3), it is observed that the permeability ratios described in Table 4 are inversely proportional to the tortuosity factor.

$$\frac{P_F}{P_U} = \frac{\Phi_P}{\tau} \tag{3}$$

where:

P_F: filled polymer permeability,
P_U: unfilled polymer permeability,
Φ_P: volume fraction of the polymer, and
τ: tortuosity factor

Considering that the volumetric fraction of the polymer on each system is the same, the possible causes that give rise to these behaviors were analyzed.

At first sight, it is noticed that transport properties improvements were not according to the order of dispersion described on TEM analyses.

PE-oC hybrid showed similar permeability rate for both gases, indicating that the phenomenon was indifferent to the penetrant gas characteristics. Evidently, this is a consequence of free volumes generated by poor interfacial adhesion. PE-oC/MP also showed similar ratios for both gases, but permeabilities values were near to pure PE values, which points out that interphase species developed a more tortuous path than the former clay.

The CH_4 permeability ratios of PE-sC, PE-oC/DP$_{Cl}$ and PE-oC/DP$_{OCH_3}$ systems were similar, despite of the differences at the PE/clay interphase. Among them, they can be mentioned the clay aspect ratio and the oligomeric species coating clays. In Figure 3, PE-sC presents an aspect ratio higher than fillers from group II, which after different treatments (cationic exchange and in situ oligosiloxane synthesis), exhibited a lower aspect ratio. Consequently, their efficiency as barrier material has been reduced. However, at the group II hybrids interphase, there are dimers that evidently equate the effects of tortuosity until reaching PE-sC permeability value.

CO_2 permeability ratios for PE-sC, PE-oC/DP$_{Cl}$ and PE-oC/DP$_{OCH_3}$ were alike, too. But permeability reduction of CO_2 was more significant than that observed to CH_4 transport. These results are probably associated with differences in gas molecule sizes or with the possible interactions that can take place between CO_2 and the organic groups at the filler surface.

About PE-oC/DM, the CH_4 permeation had a similar value to that on PE and PE-oC/MP. Nevertheless, this hybrid at CO_2 permeation exhibited an improvement in the barrier properties. Therefore, in spite of having the same interphase characteristics (free volume and oligomers), gas molecules had presented different behaviors, probably due to reasons already cited on the above paragraph.

6.2 Pervaporation

A conventional pervaporation system was used for membrane performance testing. The permeation cell consisted of two sections separated by the membrane. A porous disk was

placed to support the membrane on the low pressure side of the membrane cell. The solvent vapor permeated through the membrane because of the very low pressure (vacuum) on the permeate side. The permeate was condensed in a trap cooled in liquid nitrogen. Measurements were carried out at 50, 60 and 70°C.

First, an analysis of PE-filler interaction was performed, and for that task values at 50°C were employed (Figure 10), as it is considered that the interactions effect at the interface will predominate over the temperature effect. PE-oC/DP$_{Cl}$ showed similar values to that of unmodified polymer. While PE-sC and PE-oC/DM exhibited better barrier properties. The remaining composites showed permeabilities above PE. In particular, PE-oC/MP and PE-oC/DP$_{OCH_3}$, which in TEM micrographs presented higher dispersion degree, showed the highest permeabilities. These results reveal that the inorganic filler dispersion is not the only factor that affects solvent transport through a polymeric membrane, but also interphase species that interact with cyclohexane molecules (Nielsen, 1967).

This analysis was extended by assessing the composite behaviors at different temperatures. Results are displayed in Figure 10.
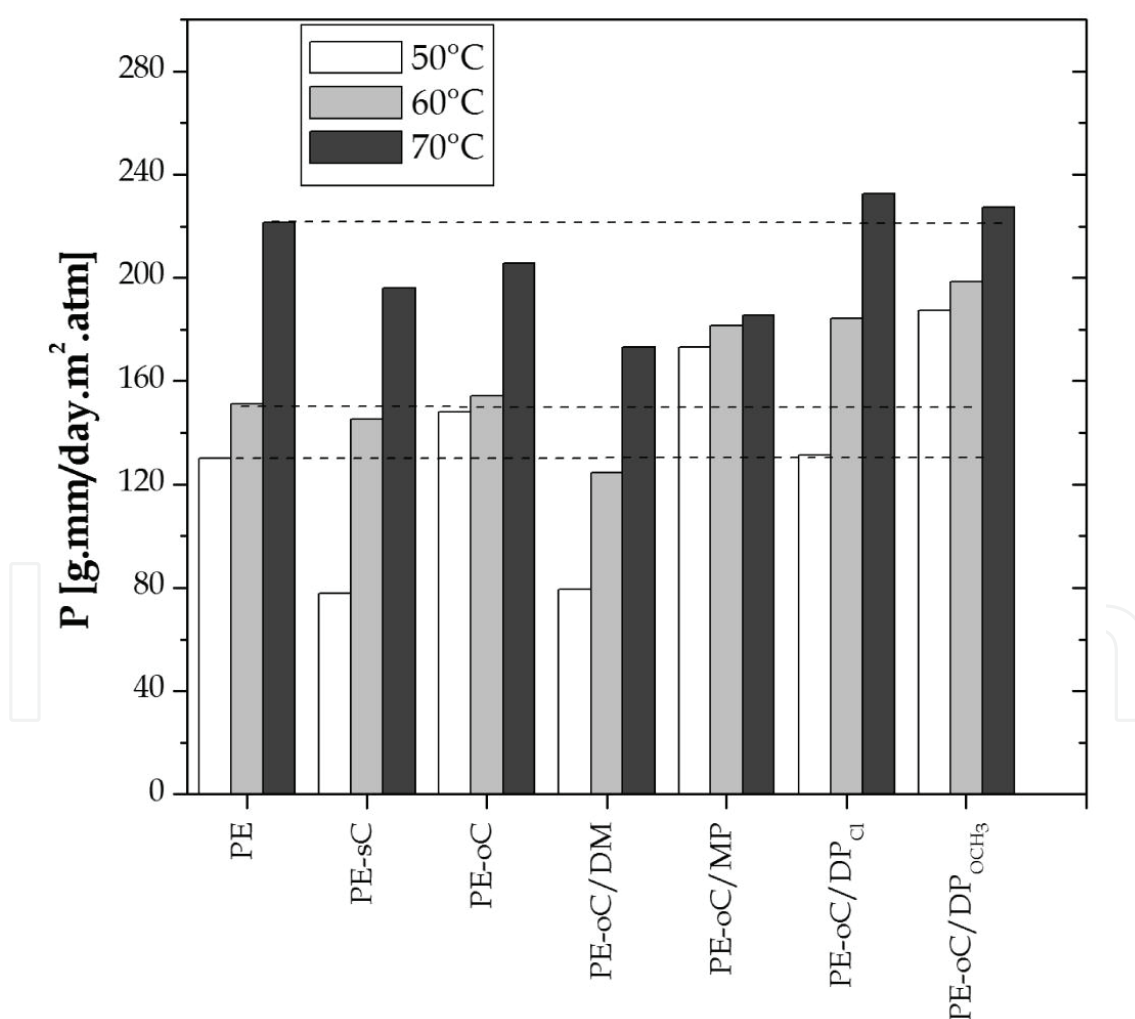

Fig. 10. Permeability coefficients of the prepared composites, compared to PE polymer (Monasterio & Destéfanis, 2011).

In order to compare the temperature effects, dashed lines taking PE values as references were pointed out. By doing so, it is possible to remark that, for each temperature, permeabilities do not increase at the same proportion for each system. This evidences different temperature sensitivities and these behaviors are closely linked to Activation Energy of Permeation (E_P). To complement this information, solubility values were determined at different temperatures which allowed calculating the Heat of Solution (ΔH_S). Finally, the Activation Energy of Difusion (E_D) is obtained by Equation 4 (Koros, 1990):

$$E_P = E_D + \Delta H_S \tag{4}$$

With the values summarized in Table 5 it is possible to split the information hidden in E_P.

	E_P [kJ/mol]	ΔH_S [kJ/mol]	E_D [kJ/mol]
PE	24.45	-11.51	35.96
PE-sC	42.68	-19.20	61.88
PE-oC	14.99	-16.42	31.41
PE-oC/DM	36.00	-12.46	48.46
PE-oC/MP	3.14	-12.64	15.78
PE-oC/DP$_{Cl}$	26.32	-19.16	45.48
PE-oC/DP$_{OCH_3}$	8.87	-14.50	23.37

Table 5. Values of activation parameter, E_D, E_P and ΔH_S.

All hybrids showed an exothermic behavior for cyclohexane solubilization. By means of ΔH_S it was observed that PE/filler systems containing oligosiloxane treated clays with side group –CH$_3$ had responses similar to PE. However, pristine clay (sC) and oC/DP$_{Cl}$ clay, which contain low concentration of oligomeric species at the surface, presented a similar behavior when interacting with the solvent. The remaining hybrids exhibited intermediate values.

The highest E_D value corresponds to the polymer with sodium clay, probably due to the tortuosity effect already mentioned in gas permeation. Hybrids with high degree of clay dispersion (PE-oC/MP y PE-oC/DP$_{OCH_3}$) presented the lowest Ed values. This tendency is associated with that proposed on reversing Cp analysis (Figure 9), where the behaviors observed where related to the mobility at the interphase, which according to the curves would be higher for PE-oC/MP and PE-oC/DP$_{OCH_3}$.

7. Discussion

In view of these results it can be stated that transport properties were affected by the structural changes on each material. According to observations in polymer-clay composites, barrier properties diminish when clay dispersion increases (Sinha Ray & Okamoto, 2003). However, although some of the hybrids herein studied presented good dispersion, they do not always present transport properties improvements.

On the other side, through DSC and rheological analysis it was noticed a plasticizing effect that was detected by the low crystallinity percentage and the decrease in viscosity,

respectively. In the papers mentioned above (X. Zheng & Wilkie, 2003; J. Zhang et al., 2005; C. Zhao et al., 2004), the treatments carried out on clay also give rise to a plasticizing effect on the polymeric matrices. Consequently, it would be expected that hybrids barrier properties were below than HDPE values. Nonetheless, behaviors were observed which did not follow this tendency and that required the consideration of the incidence of other factors for the composites analysis.

Hybrids presented similar behaviors for gas permeation, but these tendencies were not the same for cyclohexane. Specifically, PE-oC/MP and PE-oC/DP$_{OCH_3}$ seem to have reached better polymer-filler compatibility according to Cole-Cole plot (Figure 6), polar coordenates representation (Figure 4), the van Gurp-Palmen plot (Figure 7) and DSC curves (Figure 8), where those hybrids exhibited similar behaviors to that of pure PE, and both composites showed better dispersion/distribution on TEM images. Nevertheless, regarding gas transport, PE-oC/DP$_{OCH_3}$ exhibited improvements in barrier properties, while PE-oC/MP had values near to PE. But for C_6H_{12} transport both hybrids showed poor barrier properties, compared to unmodified polymer.

These responses can be explained by taking into account ´tortuosity´ (τ) and 'chain immobilization' (β) factors, which in spite of being defined for pure polymers, will be applied to the composites herein studied. τ value considers flow hindrance provoked by the increased effective length path as well as variations in the cross sectional area of the transport regions.
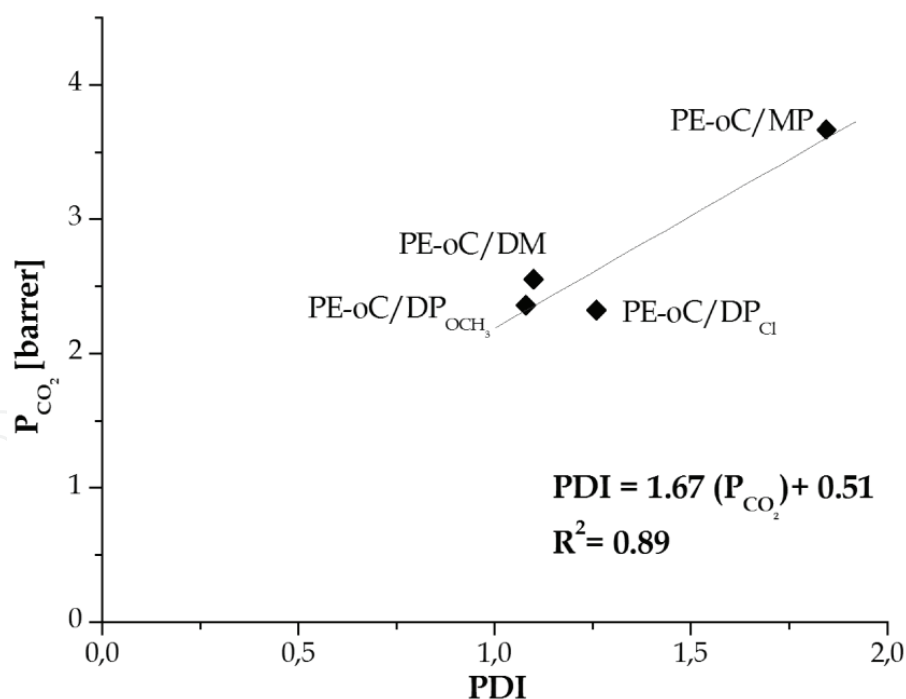

Fig. 11. Oligomers polydispersion effects on CO$_2$ permeation (For PE-oC/MP, PDI is an average value).

While β indirectly reflects the amount of increase in activation energy of diffusion caused by 'anchoring' effect from crystalline phase dispersed in amorphous phase (Koros, 1990). The diffusing species size will affect these factors in different proportions. As the sizes of the

molecules employed to determine transport properties are different (Volumes [Å^3] CH_4=27.0 < CO_2=30.7 < C_6H_{12}=101.0) (Laso & Perpète, 2006), it would be expected that for small molecules (e.g. CH_4) predominates the tortuosity effect, and while the molecule size increases the chain immobilization factor will gain importance.

Due to the hybrids contain several components, τ and β will also experiment changes related to the size and shape of oligomer side groups, and to the oligomer-oligomer and oligomer-PE interactions. According to chemical nature and spatial arrangement (or oligomer flexibility), they will affect the hybrids responses in different ways. In HDPE, crystalline domains had a 'crosslinking' effect (Koros, 1990) which prevents chain mobility on the amorphous phase.

When PE is modified with clays, although the inorganic filler inhibit chain mobility, the resulting holes from the low adhesion or the structural differences of oligomeric species would promote the amorphous phase. All factors here mentioned would explain the reason why in spite of being the same PE/clay hybrid, the transport properties behaviors in front of different molecules are not the same.

With the data obtained from each material internal structure, an analysis of the possible relations among them it will be performed. Several models have been proposed to explain and predict polymers transport properties (Koros, 1990). Nevertheless, permeability through filled polymers is very complex and the possibility of developing a model that contemplates all factors is remote (Nielsen, 1967). Thereby, they are proposed correlation that could be used in further researches.

In the hybrids containing silane modified clays, dependence between CO_2 permeability and oligosiloxane polydispersions it was found (Figure 11). Unlike CH_4 and C_6H_{12} permeabilities which would indicate that these molecules transport through these hybrids does not depend on PDI, or that this factor is uncovered by others.

For cyclohexane transport, a correlation between the crystallinity percentage and the Enthalpy of Solubility was observed. Figure 12 exhibits the mentioned correlation. Some authors (Koros, 1990) have established a link between crystallinity and solubility. Changes in the degree of crystallinity for a semicryslalline material modifies solubility because both values depend on the cohesion achieved by the species on the system (Kaufman & Falcetta, 1977), and by means of these results it was observed that the fillers used affected the molecular interactions and they were manifested on the solvent solubilization process.

Finally, the possible relations among transport properties and rheological parameters were evaluated. There were not relations describing cyclohexane behavior. However, gas permeabilities offered interesting responses for hybrids containing oC clay, as it is shown in Figure 13. Values of G' slope at the terminal zones were more related to CH_4 permeability than CO_2 permeability.

Figure 14 shows the relations detected between relative permeabilities and G_N^0/G_{cop}. In the paper of García-Franco et al. (2006), it was observed that G_N^0/G_{cop} value allows splitting the PE rheological response from copolymer composition and tends to a constant value that can be implicated with the matrix behavior in front of species of the same chemical nature. From the proposed correlations, it could be said that slope and y intercepts provide information about gas transport through the matrix and dispersed inorganic filler. G_N^0/G_{cop} would bring information about structural changes caused by compatibilizing species (changes at the interphase).

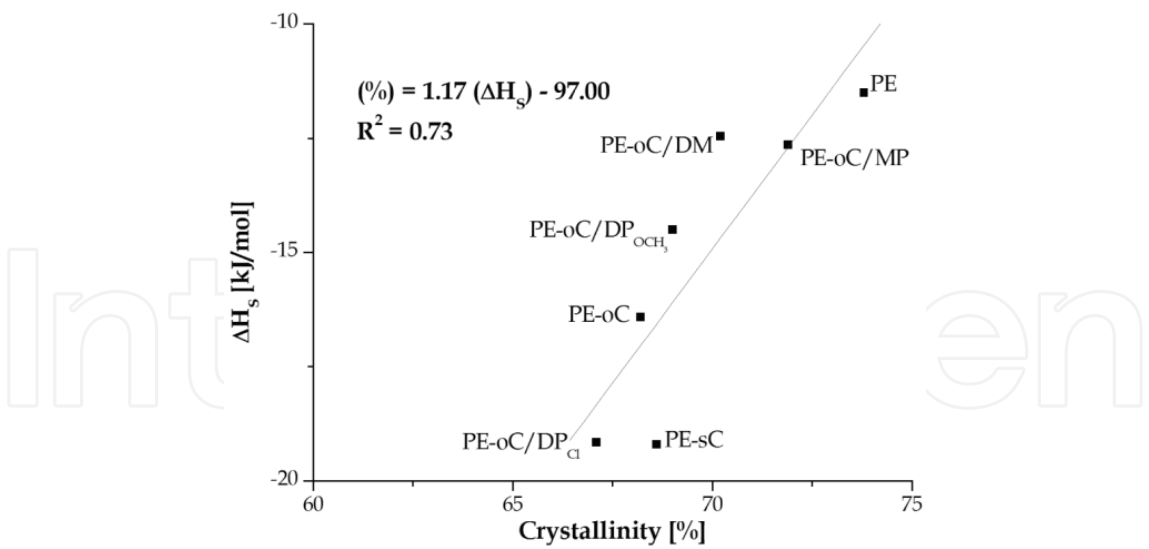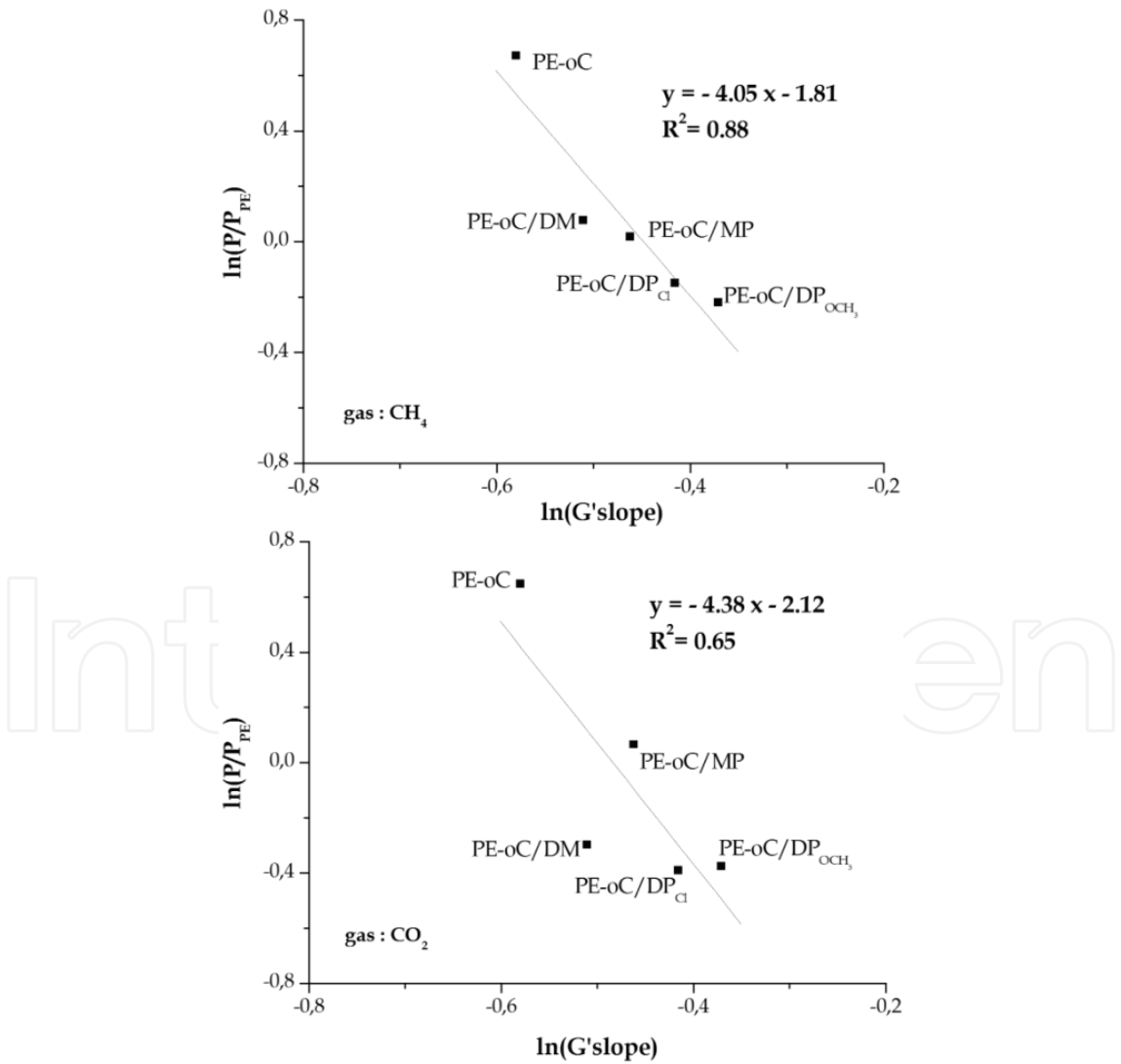Fig. 12. Degree of crystallinty vs. Enthalpy of Solubility.

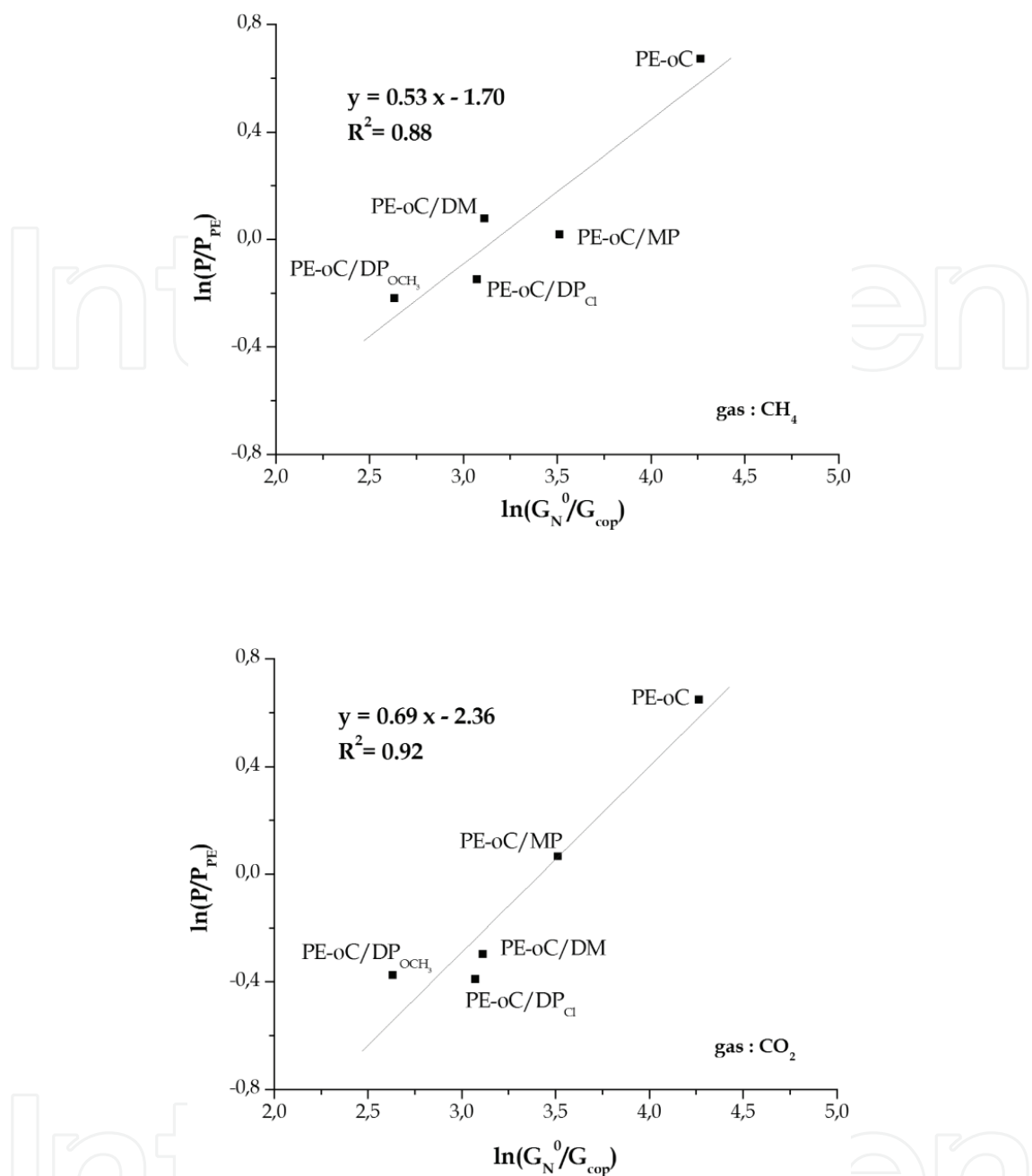Fig. 13. Comparison of CH_4 and CO_2 permeabilities with G′ slopes.

Fig. 14. Correlations founded between transport properties and rheological parameters for both gases.

As relative permeabilities are related with the tortuosity factor, a power law relationship (Equation 5) (Koros, 1990) was taken as reference aiming to explain the results.

$$\tau = \Phi^{-n} \tag{5}$$

where:

τ: tortuosity factor
Φ: amorphous volume fraction
n: exponent factor

In this expression, the crystallinity degree (related to Φ) would be describing the structural changes in the system. But, as it was noticed by modulated DSC, this value does not entirely describe the hybrids global behavior. Therefore, it is proposed the adimensional value G_N^0/G_{cop}, as each value involves several features of the systems. Taking into account that chain immobilization factor (β) can improve the interpretation of permeation in semicrystalline polymers, the following expression is suggested (Equation 6):

$$\tau.\beta = \left(\frac{G_N^0}{G_{cop}} \right)^{-n} \tag{6}$$

Certainly this equation is very simply considering the amount of factors above mentioned and it must be assessed in other system to prove their true validity.

8. Conclusions

By means of the characterizations obtained from TEM, rheology and DSC, changes in the original internal structure of HDPE were registered and this is due to the modifications caused on PE- clay intephases.

Although Transmission Electron Microscopy is a powerful technique in the detection of internal structures of filled polymers, when it was used with rheological and DSC analyses, it allow to improve the interpretation of the factors influencing the final behavior at a macroscopic level. Especially, when studying the barrier properties, as their components get into contact with the new species that diffuse through the system.

Particularly, for the hybrids from this work (groups I and II), the modulated DSC analyses and the dynamic oscillatory shear measurements lead to detect a plasticizing effect that was not perceived by TEM photographs.

Therefore, barrier properties of a system with a high degree of clay dispersion (corresponding to high filler-polymer compatibility) depend on a factor that it is not directly seen by TEM and it is the nanostructural behavior at the interphase (chain arrangement and chemical affinity between matrix and the species used as compatibilizers). This was evidenced by the group II composites (PE-oC/DP_{Cl} and PE-oC/DP_{OCH_3}), since both interphases contain oligomers of the same length and chemistry. However, differences during silane treatment affected further matrix interactions (macromolecules arrangement) and this led to differences in the responses obtained from the applied techniques.

In addition, the use of MDSC technique allowed to distinguish changes that were not detected by the conventional DSC signal.

Finally, taking into account that clay dispersion into apolar matrices (polyolefins) has been considered a critical problem, the proposed compatibilization path offers an alternative to traditional procedures. With the advantage that, by changing oligosiloxane side groups, it is possible to modify interphase behavior using low filler percentage to achieve tailor-made materials with different bulk properties.

9. Acknowledgements

10. References

Ahmed, J., Varshney, S.K., Auras, R. & Hwang, S.W. (2010). Thermal and Rheological Properties of L-Polylactide/Polyethylene Glycol/Silicate Nanocomposites Films. *Journal of Food Science*, Vol. 75, No. 8, pp. 97-108.

Alexandre, M. & Dubois, P. (2000). Polymer-layered silicate nanocomposites: preparation, properties and uses of a new class of materials. *Materials Science and Engineering*, Vol. 28, pp. 1-63.

Billmeyer, F. (Ed.). (1988). *Ciencia de los polímeros*, Reverté S.A., España.

Bretas, R.E.S. & D'Avila, M.A. (2000). *Reologia de Polímeros Fundidos*, Editorial UFSCar, Brasil.

Campbell D. & White, J. R. (1989). *Polymer Characterization, Physical Techniques*. Chapman and Hall, ISBN: 0412271605, UK.

Cassagnau, P. (2008). Melt rheology of organoclay and fumed silica nanocomposites. *Polymer*, Vol. 49, pp. 2183-2196.

Chen, D., Yang, H., He, P. & Zhang, W. (2005). Rheological and extrusion behavior of intercalated high-impact polystyrene/organomontmorillonite nanocomposites. *Composites Science and Technology*, Vol. 65, pp. 1593-1600.

Coleman, N.J. & Craig, D.Q.M. (1996). Modulated temperature differential scanning calorimetry: a novel approach to pharmaceutical thermal analysis. *International Journal of Pharmaceutics*, Vol. 135, pp. 13-29.

De Meuter, P., Rahier, H. & Van Mele, B. (1999). The use of modulated temperature differential scanning calorimetry for the characterisation of food systems. *International Journal of Pharmaceutics*, Vol. 192, pp. 77–84.

Durmus, A., Kasgoza, A. & Macosko, C.W. (2007). Linear low density polyethylene (LLDPE)/clay nanocomposites. Part I: Structural characterization and quantifying clay dispersion by melt rheology. *Polymer*, Vol. 48, No.15, pp. 4492-4502.

Faker, M., Razavi Aghjeh, M.K., Ghaffari, M. & Seyyedi, S.A. (2008). Rheology, morphology and mechanical properties of polyethylene/ethylene vinyl acetate copolymer (PE/EVA) blends. *European Polymer Journal*, Vol. 44, pp. 1834-1842.

Franck, A. (n.d.). Mixing Rules for Complex Polymer Systems, AN008e, *TA Instruments*.

Gacitua E., W., Ballerini A., A. & Zhang J. (2005). Polymer nanocomposites: synthetic and natural fillers a review. *Ciencia y tecnología*, Vol. 7, No.3, pp. 159-178.

García-Franco, C.A., Harrington, B.A. & Lohse, D.J. (2006). Effect of Short-Chain Branching on the Rheology of Polyolefins. *Macromolecules*, Vol. 39, pp. 2710-2717.

Gupta, R.K. & Bhattacharya, S.N. (2008). Polymer-clay Nanocomposites: Current Status and Challenges. *Indian Chemical Engineer*, Vol. 50 No. 3, pp. 242-267

Kaufman, H.S. & Falcetta, J.J. (1977). *Introduction to Polymer Science and Technology* (1st edition), John Wiley & Sons Inc, ISBN: 978-0471014935, USA.

Kim, B.C. & Lee, S.J. (2008). Silicate dispersion and rheological properties of high impact polystyrene/organoclay nanocomposites via in situ polymerization. *Korea-Australia Rheology Journal*, Vol. 20, No. 4, pp. 227-233.

Koros, W.J. (Ed.).(1990). *Barrier Polymers and Structures*, American Chemical Society, USA.

Laso, M & Perpète, E.A. (2006). *Multiscale modeling of polymer properties*, Elsevier, UK.

LeBaron, P.C., Wang, Z., & Pinnavaia, T.J. (1999). Polymer-layered silicate nanocomposites: an overview. *Applied Clay Science*, 15, pp. 11–29

Lee, I.B., Son, H.H., Um, C.M. (2003). Rheological properties of flowable, conventional hybrid, and condensable composite resins. *Dental Materials*, Vol. 19, pp. 298–307.

Lohse, D. J., Milner, S. T., Fetters, L. J., Xenidou, M., Hadjichristidis, N., Mendelson, R. A., García-Franco, C. A. & Lyon, M. K. (2002). Well-Defined, Model Long Chain Branched Polyethylene. 2. Melt Rheological Behavior. *Macromolecules*, Vol. 35, pp. 3066-3075.

Mai, Y.-W. & Yu, Z.-Z. (Eds.). (2006). *Polymer nanocomposites*, CRC Press, USA.

Malucelli, G., Ronchetti, S., Lak, N., Priola, A., Dintcheva, N.T. & La Mantia, F.P. (2007). Intercalation effects in LDPE/o-montmorillonites nanocomposites. *European Polymer Journal*, Vol. 43, pp. 328-335.

Michler, G.H. (2008). *Electron Microscopy of Polymers*, Springer, Germany.

Monasterio, F., Rodriguez Pita, V., Lopes Dias, M., Erdmann, E. & Destéfanis, H. (2011). Thermal and rheological properties of polyethylene composites based on poly(diphenylsiloxanes)/organoclay hybrids obtained from two different silanes. *Macromolecular Symposia*, Vol. 299/300, pp. 81–91.

Monasterio, F., Lopes Dias, M., Rodriguez Pita, V., Erdmann, E. & Destéfanis, H. (2010). Effect of the organic groups of difunctional silanes on the preparation of coated clays for olefin polymer modification. *Clay Minerals*, Vol. 45, pp. 489-502.

Monasterio, F.E. & Destéfanis, H.A. (2011). Synthesis of additives from montmorillonite to modify high density polyethylene final properties. *Macromolecular Symposia*, Vol. 301, No.1, pp. 104–113.

Nielsen, L.E. (1967). Models for the permeability of filled polymer systems. *Journal of Macromolecular Science,* Vol. A1, No.5, pp. 929-942.

Okamoto, M. (2005). Biodegradable Polymer/Layered Silicate Nanocomposites: A Review. In: *Handbook of Biodegradable Polymeric Materials and Their Applications*, Mallapragada, S. & Narasimhan, B., pp. 1-45, American Scientific Publishers, ISBN: 1-58883-053-5, USA.

Punnarak, P., Tantayanon S. & Tangpasuthadol, V. (2006). Dynamic vulcanization of reclaimed tire rubber and high density polyethylene blends. *Polymer Degradation and Stability*, Vol. 91, pp. 3456-3462.

Rose, J.M., Cherian, A.E., Lee, J.H., Archer, L. A., Coates G.W. & Fetters, L.J. (2007). Rheological Behavior of Chain-Straightened Poly(α-olefin)s. *Macromolecules*, Vol. 40, No.19, pp 6807–6813.

Rothon, R.N. (2003). *Particulated-filled polymer composites (2nd edition)*. Smithers Rapra Publishing, ISBN: 978-1859573822, USA.

Schawe, J.E.K. (1995). A comparison of different evaluation methods in modulated temperature DSC. *Thermochimica Acta*, Vol. 260, pp. 1-16.

Schlatter, G., Fleury, G. & Muller, R. (2005). Fourier Transform Rheology of Branched Polyethylene: Experiments and Models for Assessing the Macromolecular Architecture. *Macromolecules*, Vol. 38, pp. 6492-6503.

Shah, R.K. & Paul, D.R. (2004). Nylon 6 nanocomposites prepared by a melt mixing masterbatch process. *Polymer*, Vol. 45, pp. 2991–3000.

Sinha Ray, S., Bousmina, M. (2005). Biodegradable polymers and their layered silicate nanocomposites: In greening the 21st century materials world. *Progress in Materials Science,* Vol. 50, pp. 962–1079

Sinha Ray, S. & Okamoto, M. (2003). Polymer/layered silicate nanocomposites: a review from preparation to processing. *Progress in Polymer Science*, Vol. 28, pp. 1539–1641.

TA Instruments (n.d.). Measurement of Aging Effects on Amorphous Pet, TS-25.

TA Instruments (n.d.). Rheology Software Models (Flow), RN-9B. Rheology applications note.

Thomas, L.C. (2005). Why Modulated DSC? An Overview and Summary of Advantages and Disadvantages Relative to Traditional DSC. *TA Instruments*

Tobolsky, A.V. & Mark, H. (Eds.). (1971). *Polymer Science and Materials*, John Wiley & Sons, Inc., USA.

Verdonck, E., Schaap, K. & Thomas, L.C. (1999). A discussion of the principles and applications of Modulated Temperature DSC (MTDSC). *International Journal of Pharmaceutics*, Vol. 192, pp. 3–20.

Wan, C., Zhang, Yong & Zhang, Yinxi (2004). Effect of alkyl quaternary ammonium on processing discoloration of melt-intercalated PVC-montmorillonite composites. *Polymer Testing*, Vol. 23, pp. 299-306.

Wang, K.H., Choi, M.H., Koo, C.M., Xu, M., Chung, I.J., Jang, M.C., Choi, S.W. & Song, H.H. (2002). Morphology and Physical Properties of Polyethylene/Silicate Nanocomposite Prepared by Melt Intercalation. *Journal of Polymer Science: Part B: Polymer Physics*, Vol. 40, pp. 1454–1463.

Wang, L. & Sheng, J. (2005). Preparation and properties of polypropylene/org-attapulgite nanocomposites. *Polymer*, Vol. 46, pp. 6243-6249.

Williams,D. & Carter, C.B. (2009) *Transmission Electron microscopy* (2nd), Springer, ISBN, New York.

Yang, Q., Chung, T.-S., Weber, M. & Wollny, K. (2009). Rheological investigations of linear and hyperbranched polyethersulfone towards their as-spun phase inversion membranes' differences. *Polymer*, Vol. 50, pp. 524-533.

Zhang, J., Jiang, D. & Wilkie, C. (2006). Thermal and flame properties of polyethylene and polypropylene nanocomposites based on an oligomerically modified clay. *Polymer Degradation and Stability*, Vol. 91, No.2, pp. 298-304.

Zhang, Q., Yang, H. & Fu, Q. (2004). Kinetics-controlled compatibilization of immiscible polypropylene/polystyrene blends using nano-SiO2 particles. *Polymer*, Vol. 45, pp. 1913–1922.

Zhao, C., Feng, M., Gong, F., Qin, H. & Yang, M. (2004). Preparation and characterization of polyethylene-clay nanocomposites by using chlorosilane-modified clay, *Journal of Applied Polymer Science*, Vol. 93, pp. 676-680.

Zheng, X. & Wilkie, C.A. (2003). Nanocomposites based on poly (ε-caprolactone) (PCL)/clay hybrid: polystyrene, high impact polystyrene, ABS, polypropylene and polyethylene. *Polymer Degradation and Stability*, Vol. 82, pp. 441–450.
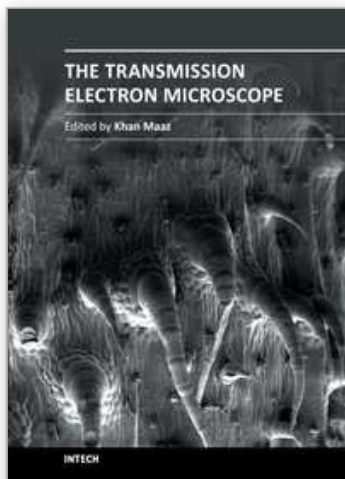
The book "The Transmission Electron Microscope" contains a collection of research articles submitted by engineers and scientists to present an overview of different aspects of TEM from the basic mechanisms and diagnosis to the latest advancements in the field. The book presents descriptions of electron microscopy, models for improved sample sizing and handling, new methods of image projection, and experimental methodologies for nanomaterials studies. The selection of chapters focuses on transmission electron microscopy used in material characterization, with special emphasis on both the theoretical and experimental aspect of modern electron microscopy techniques. I believe that a broad range of readers, such as students, scientists and engineers will benefit from this book.

How to reference
In order to correctly reference this scholarly work, feel free to copy and paste the following:

INTECH
open science | open minds